



Getting the best out of capillary electrophoresis and capillary electrophoresis–mass spectrometry by quantifying sources of peak broadening for proteins using polyelectrolyte multilayer coated fused silica capillaries

Laura Dhellemmes, Laurent Leclercq, Alisa Höchsmann, Christian Neusüß, Michel Martin, Hervé Cottet

► To cite this version:

Laura Dhellemmes, Laurent Leclercq, Alisa Höchsmann, Christian Neusüß, Michel Martin, et al.. Getting the best out of capillary electrophoresis and capillary electrophoresis–mass spectrometry by quantifying sources of peak broadening for proteins using polyelectrolyte multilayer coated fused silica capillaries. *Analytical Chemistry*, 2024, 96 (38), pp.15205-15212. 10.1021/acs.analchem.4c02276 . hal-04731244

HAL Id: hal-04731244

<https://hal.science/hal-04731244v1>

Submitted on 13 Oct 2024

HAL is a multi-disciplinary open access archive for the deposit and dissemination of scientific research documents, whether they are published or not. The documents may come from teaching and research institutions in France or abroad, or from public or private research centers.

L'archive ouverte pluridisciplinaire **HAL**, est destinée au dépôt et à la diffusion de documents scientifiques de niveau recherche, publiés ou non, émanant des établissements d'enseignement et de recherche français ou étrangers, des laboratoires publics ou privés.

Getting the best out of CE and CE-MS by quantifying sources of peak broadening for proteins using polyelectrolyte multilayer coated fused silica capillaries

Laura Dhellemmes¹, Laurent Leclercq¹, Alisa Höchsmann^{2,3}, Christian Neusüss², Michel Martin⁴,
Hervé Cottet^{1*}

¹ IBMM, University of Montpellier, CNRS, ENSCM, Montpellier, France

² Faculty of Chemistry, Aalen University, 73430 Aalen, Germany

³ Faculty of Science, Eberhard Karls University Tübingen, 72074 Tübingen, Germany

⁴ PMMH, CNRS, ESPCI Paris-PSL, Sorbonne Université, Université de Paris, 75005 Paris, France

ABSTRACT: Capillary electrophoresis (CE) has emerged as a relevant technique for protein and biopharmaceutical analysis, as it combines high separation efficiency, sensitivity and versatility. The use of capillary coatings, including successive multiple ionic-polymer layers (SMIL), reduces interactions between analytes and the capillary, further improving CE performance. Nevertheless, separations done on SMIL coatings rarely surpass 500×10^3 plates/m. In order to obtain the best out of CE, it is interesting to have a detailed look at the sources of peak dispersion. Separations of a mix of model proteins were performed on (poly(diallyldimethylammonium chloride)/poly(styrene sulfonate))_{2.5} coated capillaries at different electric field strengths, leading to plate height H against migration velocity u plots which enabled a quantitative analysis of each contribution. Using this model, capillary lengths and injected volumes were systematically varied. For the first time, the contribution of sample electrophoretic heterogeneity to the total peak dispersion was deciphered for model proteins and a monoclonal antibody. Dispersion due to electromigration was seen to have an impact on plate heights in the case of triangular peaks of small molecules but not for proteins in the present conditions. UV and mass spectrometry detection were compared on the same capillary, providing valuable information on the impact of the detection type on separation efficiency. Close to 1 million plates/m were reached in the best conditions.

Introduction

As therapeutic proteins have come to represent an increasingly large part of the pharmaceutical market, their characterization has become all the more important. Biopharmaceuticals such as monoclonal antibodies (mAbs), hormones, fusion proteins, and vaccines, are being developed for the treatment of various illnesses such as cancer, cardiovascular diseases, diabetes, and autoimmune disorders, against which they are sometimes more effective than their small molecule counterparts ^{1,2}. In addition, biosimilars are created once patents expire, resulting in similar compounds which most likely differ from the original drug in some way, due to their high complexity and biological source ³. These variations must be monitored to ensure product safety and efficiency, requiring precise and robust analytical methods. Among these, capillary electrophoresis (CE) is an effective

separation technique well suited to the analysis of both small molecules and proteins, due to its high separation efficiency and different selectivity as compared to chromatographic techniques. It separates analytes based on their charge and size, making it interesting for characterizing sample charge heterogeneity. Moreover, in the ideal case, separation efficiency is inversely proportional to the analyte's diffusion coefficient, and so, CE is supposed to be particularly efficient for large molecule analysis ⁴. Several applications of CE for the separation of mAb charge variants have been reported, often using ϵ -aminocaproic acid (EACA) as an additive to improve the separation efficiency and selectivity ^{5 6 7 8 9 10 11} or Good's buffers ¹².

In order to improve separation efficiency and reproducibility of CE methods, coatings may be applied to the inner surface of the capillary. Among these, successive

multiple ionic-polymer layers (SMIL) are made from depositing polyelectrolyte layers onto the capillary surface, alternating between polycationic and polyanionic solutions which are linked through electrostatic interactions^{13,14}. They provide a charged surface generating relatively strong electroosmotic flow (EOF) and reduce adsorption of analytes with the same type of charge (negative or positive) as the last SMIL layer. They are particularly useful for analyzing peptides and proteins^{15,16,17,18}. The improved reproducibility compared to uncoated capillaries allows coupling of CE with mass spectrometry (MS) as long as some experimental conditions are respected, such as choosing a volatile background electrolyte (BGE) and a EOF direction toward the mass detector¹⁹. CE-MS has been successfully applied for the separation of mAb charge variants, becoming one of the most widely used technique for intact protein analysis^{4,20,21}. It enables compound identification in addition to better selectivity, and is also compatible with the use of SMIL coatings, which are stable enough to not interfere with MS detection²².

With the goal of improving CE performance, efforts to better understand the parameters influencing separation efficiency have been made. Different models of peak dispersion in CE have been proposed, including the plate height against migration velocity plot, which was first introduced to CE by Minarik et al.²³, similarly to the Van Deemter equation used in chromatography:

$$H = \frac{B}{u} + pu + \text{constant} \quad (1)$$

The $\frac{B}{u}$ term corresponds to axial diffusion and is expressed as $H_{DA} = \frac{2D}{u}$, where D is the analyte diffusion coefficient^{24,25,26,27}. The pu term corresponds to the linear ascending part of the curve, and has been attributed to analyte adsorption^{23,25} or to inhomogeneities in coating charge, and thus in local EOF²⁸. Sample adsorption onto the capillary wall has been widely accepted as one of the main limiting factors to high separation efficiency. The influence of solute adsorption on H in CE was modelled assuming a fast equilibrium of the solute with the capillary surface as in the theory of chromatography with however a different velocity profile^{23,25}. Carrying out model protein separations at different electric field strengths and measuring the resulting plate heights enabled to plot the H vs u curve and to determine the slope p of the ascending part²⁵. This model was refined in a later publication proposing the addition of a constant term to take into account effects which do not depend on the electric field strength²⁹. Further investigations about the origin of the slope revealed that adsorption involving a small number of sites onto the capillary surface and slow kinetics of desorption may be more relevant than the previous retention-based model²⁸. Electroosmotic flow inhomogeneity due to coating defects has also been shown to contribute to the slope p ²⁸. In addition, sample injection, detection, capillary coiling, electromigration dispersion (EMD) and temperature gradients have been cited as possible sources of dispersion^{29,30,31}. Nevertheless, thorough and quantitative investigations of all the contributions to peak dispersion in CE using SMIL coatings,

including those due to extra-column effects responsible for the constant term, are still lacking.

To get the best performances in CE, and to try to reach plate numbers close to the maximal theoretical values obtained if we consider that the only source of dispersion is axial molecular diffusion (up to four million plates/m for a protein with a diffusion coefficient of $D = 5 \times 10^{-11} \text{ m}^2\text{s}^{-1}$, a capillary length to the detector $l = 71.5 \text{ cm}$ and migration time $t_m = 20 \text{ min}$), it is necessary to precisely evaluate the contribution of each source of dispersion, and thus, to optimize all the CE experimental conditions. In this work, H vs u curves were systematically plotted for each protein by repeating experiments at different voltages. An overview of the main causes of dispersion in CE was given, including extra-column effects and detection type, resulting in better insight into the mechanisms governing separation efficiency. Particular attention was paid to the variations of the constant term in the H vs u curves. First, capillary dimensions and injection parameters were varied and their impact on separation efficiency was studied. In addition to the injection, detection and capillary coiling effects, EMD was also shown to contribute to plate height for triangular peaks. Next, UV- and MS-detection were compared in terms of separation efficiency on the same capillary. The analyses were conducted with five model proteins in a 2 M acetic acid BGE on (poly(diallyldimethylammonium chloride) (PDADMAC)/poly(styrene sulfonate) (PSS))_{2.5} coated capillaries.

Theoretical part

Among the parameters contributing to peak dispersion in CE, several of them depend on the capillary total and/or effective lengths, one of them being sample injection. Considering that the injection plug is rectangular, it can be expressed as follows²⁴:

$$H_{inj} = \frac{l_{inj}^2}{12l} \quad (2)$$

where l_{inj} is the plug length.

Knowing that the injected length is equal to

$$l_{inj} = \frac{\Delta P R^2 t_{inj}}{8\eta L} \quad (3)$$

where ΔP is the injection pressure, R the capillary internal radius, t_{inj} the injection time, η the viscosity of the BGE and L the total capillary length, we obtain:

$$H_{inj} = \frac{R^4 \Delta P^2 t_{inj}^2}{768 L^2 \eta^2 l} \quad (4)$$

The detector cell with an aperture τ_{det} also adds onto band broadening as follows:

$$H_{det} = \frac{\tau_{det}^2}{12l} \quad (5)$$

with $\tau_{det} = 620 \text{ } \mu\text{m}$ for 50 μm I.D. capillaries according to Agilent documentation. Next, capillary coiling can lead to

increased dispersion due to the difference between the migration distance of solutes on the outer and inner circumference ^{24,32,33}, and may be expressed as:

$$H_{coil} = \frac{R^2 l}{4r_{coil}^2} \quad (6)$$

where r_{coil} is the internal radius of the capillary coil. Other effects such as a radial and axial temperature gradients have been investigated ^{24,34} but are negligible in this work given the low conductivity (0.244 S/m) of the BGE.

Previous work has analyzed the contributions to the slope p and determined that some proteins are adsorbed onto the capillary wall, leading to a pu term ²⁸. In addition, the presence of heterogeneous zones on the capillary coating due to uneven coating or impurities modifies the EOF locally, which also leads to peak broadening which is dependent on u ^{28 35 36}. In the case of a step discontinuity, where one zone of the capillary of length z_a has a different charge than the rest, and where $z_a > l$, this additional plate height is expressed as ²⁸:

$$H_{EOF} = (1 - f)^2 \left(\frac{\Delta\mu_{eo}}{\mu_{eo}^0 + \mu_{ep}} \right)^2 \frac{R^2 u}{24D} \quad (7)$$

where f is the fraction of inhomogeneity equal to $f = \frac{z_a}{L}$, $\Delta\mu_{eo}$ is the difference in EOF between the two zones, μ_{eo}^0 is the mean fluid mobility, and μ_{ep} is the protein electrophoretic mobility.

In the case of a step discontinuity where $z_a < l$, the equation becomes:

$$H_{EOF} = F \left(\frac{\Delta\mu_{eo}}{\mu_{eo}^0 + \mu_{ep}} \right)^2 \frac{R^2 u}{24D}$$

with

$$F = f \frac{L}{l} + f^2 \left(1 - 2 \frac{L}{l} \right)$$

In practice, coatings which are considered homogeneous may contain many discontinuities. Assuming that these are distributed homogeneously along the capillary, the resulting plate height may be expressed as:

$$H_{EOF} = f(1 - f) \left(\frac{\Delta\mu_{eo}}{\mu_{eo}^0 + \mu_{ep}} \right)^2 \frac{R^2 u}{24D}$$

Another possible contribution to band broadening in CE is sample heterogeneity. In this next part, an expression of the additional plate height resulting from this effect will be given. The analysis by CE of a sample which is not a pure compound but a mixture of components with slightly different electrophoretic mobilities, μ , is considered. This polydispersity in mobility contributes to increase the peak broadening since the sample peak, in that case, is made of the superposition of individual peaks of the sample components with slightly different migration times which are insufficiently separated and resolved. In this section, the expression of the contribution, H_p , of the polydispersity to the plate height, H , of the peak, is determined. The distribution of electrophoretic mobilities is characterized by the average mobility and the standard deviation of the mobilities, σ_μ .

The contribution, $\sigma_{t,p}$, to temporal standard deviation, of the sample peak arising from the polydispersity is approximately estimated by the difference in migration times observed for two components whose mobilities differ by σ_μ , hence:

$$\sigma_{t,p} = \left(\frac{dt}{d\mu} \right) \sigma_\mu$$

where t is the migration time, which, in CE, is given by:

$$t = \frac{l}{\mu E} = \frac{Ll}{\mu V}$$

where E is the electrical field strength and V the voltage drop along the capillary. From Eq. 12, we obtain:

$$\frac{dt}{d\mu} = - \frac{l}{E\mu^2} = - \frac{t}{\mu}$$

To $\sigma_{t,p}$ corresponds a contribution $\sigma_{z,p}$ of the polydispersity to the spatial standard deviation of the peak equal to:

$$\sigma_{z,p} = \mu E \sigma_{t,p}$$

Hence, combining Eq. 11 to 13 gives:

$$\sigma_{z,p} = -l \frac{\sigma_\mu}{\mu}$$

Since the plate height H is equal to:

$$H = \frac{\sigma_z^2}{l}$$

where σ_z^2 is the total variance of the peak, the contribution H_p to H is given by:

$$H_p = l \left(\frac{\sigma_\mu}{\mu} \right)^2 \quad (8)$$

In this expression, the mean electrophoretic mobility of the zone, $\bar{\mu}$, should be chosen for μ .

As the overall plate height H is proportional to the variance of the distances migrated by the molecules, it is made of a sum of terms which reflect independent contributions to the overall variance. Hence the expression of H_p given by Eq. 17 appears as an additional contribution to H . This contribution to H is proportional to the square of the relative standard deviation of the distribution of the electrophoretic mobilities and to the migration distance, but independent of other operating parameters. ⁽⁹⁾

Materials and Methods

Chemicals & solutions

2-[4-(2-hydroxyethyl)piperazin-1-yl]ethane sulfonic acid (HEPES) and acetic acid were purchased from Sigma-Aldrich (Saint-Quentin Fallavier, France). The model basic proteins, i.e. Carbonic Anhydrase I from bovine erythrocytes (CA, purity not indicated by the supplier), Trypsin Inhibitor from Glycine max (soybean) (TI, purity not indicated by the supplier), Myoglobin from equine skeletal muscle (Myo, purity $\geq 95\%$), Ribonuclease A from bovine pancreas (RNase A, purity $\geq 60\%$), β -lactoglobulin

A from bovine milk (β -lac A, purity $\geq 90\%$), and Lysozyme from chicken egg white (Lyz, purity $\geq 90\%$) were purchased from Sigma-Aldrich (Saint-Quentin Fallavier, France). See Table S1 for more protein characteristics. The USP mAb003 (lot: F12980) was purchased from Sigma-Aldrich (Steinheim, Germany). Ultrapure water was obtained using a MilliQ system from Millipore (Molsheim, France). Poly(diallyldimethylammonium chloride) (PDADMAC, high molecular mass: M_r $4 \times 10^5 - 5 \times 10^5$) 20% w/w in water was purchased from Aldrich (Lyon, France). Poly(styrene sulfonate) (PSS, M_r 7×10^5) was purchased from Acros Organics (Geel, Belgium).

Coating Procedure

To prepare the SMIL coatings, the fused silica capillary was preconditioned by flushing with 1 M NaOH for 10 min, water for 5 min and HEPES for 10 min. The construction buffer used to rinse the capillary between the deposition of polyelectrolyte layers was a 20 mM HEPES solution with 10 mM NaOH at pH 7.4 ($I = 10$ mM). Polyelectrolyte solutions, 3 gL⁻¹ PDADMAC and PSS in HEPES, were prepared at least one night before the first use. These were stored in the freezer in the case of PDADMAC and in the refrigerator in the case of PSS to avoid degradation over time. The background electrolyte (BGE) used for the inlet and outlet vials and for rinsing between runs was 2 M acetic acid at pH 2.2 ($I = 6.4$ mM). These solutions were injected in glass vials containing 1 mL.

The polyelectrolyte layers were deposited by flushing with PDADMAC and PSS solutions for 7 min each, alternating between the two and flushing with HEPES for 3 min in between each one. These polyelectrolyte solutions were injected in polypropylene vials containing 0.2 mL, where the capillary is immersed in solution which is below the level of the electrodes, limiting contamination between the vials. To further reduce this possibility, different HEPES vials were used to rinse the capillary after PDADMAC and PSS flushes.

After the last HEPES flush, wait 5 min and flush with water for 3 min, with BGE for 10 min and wait for 5 min. All flushes were performed at 930 mbar. SMILs will be referred to as (A/B)_{*i*}, where A is the polycation, B the polyanion, and *i* the number of bilayers.

Capillary Electrophoresis

Analyses were performed on an Agilent 7100 CE (Waldbronn, Germany). Fused silica capillaries of 50 μ m in diameter and 30 cm to 80 cm total length were from Composite Metal Servies (Photon Lines, France). The length to the detector was equal to the total length minus 8.5 cm, except in the case where the sample was injected from the outlet side, where it was equal to 8.5 cm. Applied voltages were adjusted depending on the total capillary length to keep the same range in *u*, i.e. -30 kV to -15 kV for the 80 cm capillaries, -25 kV to -10 kV for the 60 cm capillaries, -15 kV to -7 kV for the 40 cm capillaries, and -10 kV to -5 kV for the 30 cm capillaries. They were flushed for 5 min with BGE at 930 mbar before each run. The injection parameters were adapted to the intended volume

and capillary length (see Figure 1). The analyses were done at 25°C and the UV detection at 214 nm.

The protein mix was prepared from individual solutions of proteins in water as proteins were seen to degrade over time when stored in BGE and possibly to interact with each other when stored together²⁹. These protein stock solutions at 2 gL⁻¹ could be kept in the freezer for several months without problem. Before analysis, the stock solutions were thawed and the mix was prepared from 10 μ L of each, adding 50 μ L of 4 M AcOH for a final concentration of each protein at 0.2 gL⁻¹ in a 2 M AcOH medium. The mix then underwent a heat treatment at 37°C for 30 min and was added to a polypropylene conical vial for analysis. The EOF marker was 0.002% v/v DMF in BGE, which was injected before the protein mix at a lower injection volume (typically half that of the mix).

Calculations of separation efficiencies were done with CEval software³⁷ available at [https://echmet.natur.cuni.cz/]. The capillary total (*L*) and effective (*l*) lengths must be entered in the software, as well as the half ramp time ($t_{1/2} = 0.6$ s on Agilent instruments).

Capillary Electrophoresis-Mass Spectrometry

For CE-ESI MS measurements, an Agilent 7100 CE (Waldbronn, Germany) was coupled to a maXis QTOF MS (Bruker Daltonics, Bremen, Germany) using the nanoCEasy interface³⁸ (see Figure S1). Fused silica capillaries (Separation capillary inner/outer diameter 50 μ m/360 μ m, sheath liquid capillary 100 μ m/240 μ m) were obtained from Polymicro Technologies (Phoenix, AZ, USA). For CE-MS measurements the tip of the capillary was etched to about 80-100 μ m OD applying hydrofluoric acid³⁸. Glass emitter of 30 μ m ID were obtained from BioMedical Instruments (Zöllnitz, Germany). Propan-2-ol:water (1:1) with 0.5% v/v formic acid was used as sheath liquid. Electrospray voltage was set to 2000 V. The mass range was *m/z* 400 – 3000 with a spectra rate of 1 Hz. MS data analysis was performed using DataAnalysis 4.3 (Bruker Daltonics). Extracted ion electropherograms were generated using the most intense charge state for each protein and used for determination of migration time and peak width. External UV detection was performed at 51.5 cm using an ECD2600 UV detector (ECOM spol. s r.o., Prague, Czech Republic) at a wavelength of 200 nm applying data sample rate of 10 Hz and a time constant of 0.5 s.

Results and Discussion

Impact of capillary length and injection volume in CE-UV

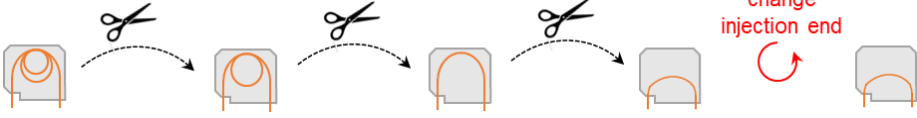
Experimental setup

To quantify the impact of capillary length and injection volume on plate heights, separations of model proteins on capillaries with different lengths and injection volumes were carried out (see Figure S2). In total, 9 series of 5

repetitions on 5 different voltages were carried out on two capillaries, which corresponds to 225 runs. To maintain exactly the same surface characteristics of the SMIL

coating, a single (PDADMAC/PSS)_{2.5} coated capillary was cut from 80 cm to 60 cm, 40 cm and then 30 cm, for each injection

Table 1. Description of experiments (5 repetitions) done on two (PDADMAC/PSS)_{2.5} coated capillaries, before and after different capillary cuts, leading to different lengths and using two injection volumes, and 5 different voltages. Experimental conditions:

					
<i>L</i> (cm)	80	60	40	30	30
<i>l</i> (cm)	71.5	51.5	31.5	21.5	8.5
<i>P</i> _{inj} (mbar); <i>t</i> _{inj} (s)	30; 4		2; 30	2; 23	2; -23
<i>V</i> _{inj} (nL)	1.9		1.9	1.9	1.9
<i>V</i> (kV)	-15; -17.5; -20; -25; -30		-5; -7; -11; -13; -15	-5; -7; -8; -9; -10	-5; -7; -8; -9; -10
<i>P</i> _{inj} (mbar); <i>t</i> _{inj} (s)	30; 8	30; 6	30; 4	30; 3	-30; 3
<i>V</i> _{inj} (nL)	3.8	3.8	3.8	3.8	3.8
<i>V</i> (kV)	-15; -17.5; -20; -25; -30	-10; -12.5; -15; -20; -25	-5; -7; -11; -13; -15	-5; -7; -8; -9; -10	-5; -7; -8; -9; -10
(PDADMAC/PSS) _{2.5} SMIL. For the coating procedure, see section 2.2. Capillary: 50 μm I.D.					

volume *V*_{inj}. Injection times and pressures were varied according to the capillary length to keep the same injected volume (see Table 1), according to the Poiseuille law:

$$V_{inj} = \frac{\Delta P \pi R^4 t_{inj}}{8 \eta L} \quad (18)$$

To further decrease the length to the detector, the sample was also injected from the other end of the capillary on a 30 cm capillary, for a detection path of 8.5 cm (entering a negative pressure from the inlet side on the Agilent system to inject from the outlet side). The different contributions, as calculated from their theoretical expressions, are summarized in Table 2 and are compared to the total experimental plate height obtained for one protein (CA), visually represented in Figure 1.

Axial diffusion

There are three terms in the dependence of *H* vs *u* curve. The 1/*u* term is related to axial diffusion and is negligible in the experimental range of *u* investigated in this work (see the location of the experimental data points in Figure 1). This means that the experimental points are located in the ascending part of the *H* vs *u* curve and that contrary to what is often assumed, axial diffusion is not controlling peak broadening in most of the practical conditions used in CE for protein separation.

Contributions to the slope

Regarding the slope *p* of the *H* vs *u* curve, a previous study demonstrated that this term is impacted by the homogeneity in charge of the coating or capillary surface for all the proteins, and possibly for some of the proteins, adsorption onto the capillary wall²⁸. In particular, CA, Myo,

RNAse and Lyz were seen to have very low slopes which were not sensitive to saturation of adsorption sites, while β-lactoglobulin A had a much higher slope (8 times higher than the average of the four others) which decreased when the analyses were done after rinsing the capillary with the protein mix or after adding the proteins to the BGE²⁸. In this work, CA, TI, Myo, RNAse, and Lyz led to similar values of *p* on a given capillary, which leads to think that they are governed by the same phenomenon, which is most likely electroosmotic inhomogeneity rather than adsorption. Some variations between proteins are nevertheless to be expected, since the *H*_{EOF} term depends on each protein's electrophoretic mobility and diffusion coefficient (see Eq. 10 and Table S2).

For equal injected volumes, a longer capillary reduces *p* and therefore the impact of surface coating inhomogeneity on peak broadening, as can be seen in the evolution of Figure 1A to Figure 1E. If coating defects are homogeneously distributed along the capillary, as described in the model, capillary length should not affect the resulting slopes. However, this is a simplified vision, and depending on the location and the distribution of the inhomogeneity within the capillary surface, the case of a step discontinuity may be more appropriate. In particular, if the heterogeneity is located before the detector, Eqs. 8 and 9 describe that *H* depends on the ratio *L*/*l*, which decreases for longer capillaries. Hence, the decline in slopes as the capillary length increases is consistent with the idea that they are controlled mainly by electroosmotic inhomogeneities.

Contributions to the constant

As to the constant contributions to H , the injection is the most important (8 to 54% of the constant depending on the capillary length and injected volume), and it increases significantly as L and l decrease, as expected by the theory since H scales as $\frac{l_{inj}^2}{l}$. Each contribution given in Table 2 was calculated for a fixed velocity u of about 5.2×10^{-4} m/s, meaning at adjusted applied voltages depending on the total capillary length to get constant electric field strength. The contributions linked to the detection window and the capillary coiling were always very low (below 14%). In Figure 1, the extra-column contribution H_{extra} which is not predicted from the different constant contributions described in the theoretical section was calculated by removing the total calculated contributions (H_{DA} from Eq. 1, H_{slope} from Eq. 1, H_{inj} from Eq. 4, H_{det} from Eq. 5, H_{coil} from Eq. 6) from the experimental constant obtained with the fitting of the H vs u curve. H_{extra} is particularly high for the 30 cm capillary injected from the outlet side ($l = 8.5$ cm), as is shown in Figure 1E and Figure 1I, which may be because

the proteins are badly separated in that case due to the very small length to the detector (see Figure S2E). It can also be noted that H_{extra} generally decreases as the injected volume decreases, which could indicate that the contribution to injection has been underestimated. Indeed, Eq. 2 describes the plate height resulting from the injection of a rectangular plug, which relies on the assumption that the sample is uniformly distributed in the cylindrical section of the capillary. This implies a very fast radial sample migration, which is the most favorable situation. If, instead, the sample radial diffusion rate was very low, the sample would then occupy a paraboloid of double the length, because of the parabolic flow profile. In practice, the situation is likely intermediate between these two cases, depending on the duration of the injection process and on the sample diffusion coefficient, which may explain a still larger contribution of the injection process to the constant than that reflected in Table 2 and Figure 1. The detailed contributions to plate height for the other proteins are shown in Figure S3 to S6.

Table 2. Contributions to plate height calculated from the theory and comparison with the experimental data for different capillary lengths and injection times. Two injection volumes were used, $V_1 = 1.9$ nL and $V_2 = 3.8$ nL. Data shown for CA at constant u obtained at -17.5 kV for the 80 cm capillaries, -12.5 kV for the 60 cm one, and -9 kV for the 40 cm and 30 cm ones. The superscripts indicate how each value was calculated. a: $u = \frac{l}{t_{apex} - t_{1/2}}$, where t_{apex} is the migration time of each protein at the peak maximum, $t_{1/2}$ is the half ramp time (0.6 s on Agilent CE); b: H_{DA} is calculated with Eq. 1; c: p is calculated with Eq. 1; d: $H_{slope} = pu$; e: H_{inj} is calculated with Eq. 4; f: H_{det} is calculated with Eq. 5; g: H_{coil} is calculated with Eq. 6; h: $H_{total,calc} = H_{DA} + H_{slope} + H_{inj} + H_{det} + H_{coil}$; i: H_{exp} is the experimental point obtained for the chosen u , calculated with $H = \frac{l}{5.54 \left(\frac{t_{apex}}{\delta} \right)^2}$, where δ is the peak width at half height; j: injection from outlet end, voltage polarity from inlet end.

V_{inj}	L (cm)	l (cm)	u (10^{-3} m/s) a	V (V)	H_{DA} (μ m) ^b	p (10^{-3} s) ^c	H_{slope} (μ m) ^d	H_{inj} (μ m) ^e	H_{det} (μ m) ^f	H_{coil} (μ m) ^g	$H_{total,calc}$ (μ m) ^h	H_{exp} (μ m) ⁱ
V ₁	80	71.5	0.51	-17500	0.188	1.48	0.76	0.11	0.04	0.12	1.23	1.84
	40	31.5	0.52	-9000	0.184	1.75	0.92	0.25	0.10	0.05	1.51	2.97
	30	21.5	0.54	-9000	0.178	2.73	1.47	0.39	0.15	0.04	2.23	3.30
	30	8.5	0.53	9000 j	0.181	4.95	2.63	0.98	0.38	0.01	4.18	15.08
V ₂	80	71.5	0.50	-17500	0.191	1.18	0.60	0.44	0.04	0.12	1.40	2.62
	60	51.5	0.48	-12500	0.199	1.29	0.62	0.62	0.06	0.09	1.59	3.19
	40	31.5	0.52	-9000	0.184	1.77	0.92	1.01	0.10	0.05	2.27	4.72
	30	21.5	0.54	-9000	0.177	6.20	3.37	1.48	0.15	0.04	5.21	6.27
	30	8.5	0.52	9000 j	0.184	17.82	9.34	3.74	0.38	0.01	13.66	23.43

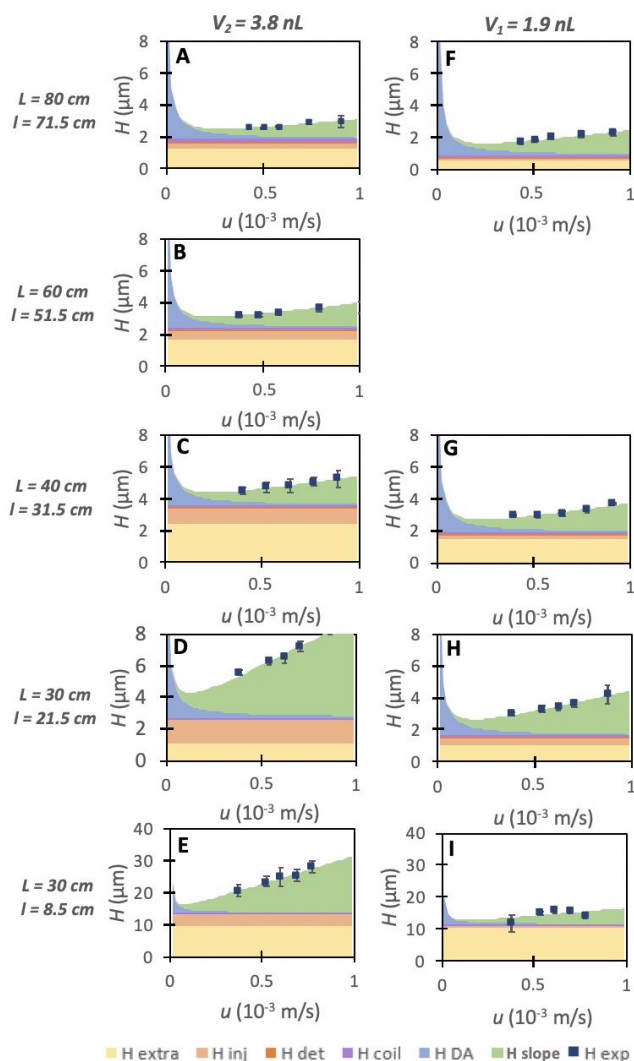


Figure 1. Visual representation of each contribution to plate height for five different capillary lengths and two injected volumes for CA. $V_2 = 3.8$ nL for $L = 80$ cm (A), $L = 60$ cm (B), $L = 40$ cm (C), $L = 30$ cm and $l = 21.5$ cm (D), $L = 30$ cm and $l = 8.5$ cm (E). $V_1 = 1.9$ nL for $L = 80$ cm (F), $L = 40$ cm (G), $L = 30$ cm and $l = 21.5$ cm (H), $L = 30$ cm and $l = 8.5$ cm (I). Error bars are \pm one standard deviation on 5 runs. Experimental conditions: 5-layer PDADMAC/PSS SMIL coated capillary. Capillary: 50 μ m I.D. BGE: 2 M acetic acid, pH 2.2. Flush before each run: BGE 1 bar, 5 min. Sample mixture: 0.2 g/L of CA, TI, Myo, RNase A, and Lyz each in BGE. Hydrodynamic co-injection of 0.002% v/v DMF in BGE: half the amount of injection protein mix. Temperature: 25°C. For the coating procedure, see section 2.2.

It was possible to significantly reduce the injection contribution to the plate height by decreasing the injection volume by a factor of 2 (see Figure 1A to 1E vs Figure 1F to 1I). In the best-case scenario (Figure 1F: 80 cm capillary, small injection volume V_1 , low electric field strength -15 kV), plate heights reached as low as 1.06 μ m (for Myo), which corresponds to 941×10^3 plates/m. Figure 2 shows the corresponding electropherograms, which highlight both the excellent repeatability of the runs, which are indistinguishable from each other at one electric field strength, as well as the high separation efficiency. Indeed,

the protein peaks appear to be very thin and some small satellite peaks surrounding the main peaks can be seen due to the excellent separation efficiency.

For reference, the highest separation efficiency obtained with a SMIL thus far was 803×10^3 plates/m (for Cytochrome C with 13-layer PDADMAC/PSS)³⁹, with most averaging around 100 to 500×10^3 plates/m (for various model proteins)⁴⁰. Therefore, increasing capillary length or reducing injection volume is a definite way of improving separation efficiency.

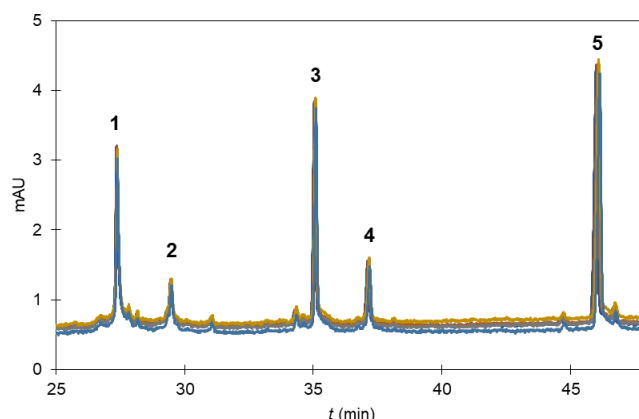


Figure 2. Electropherograms for the separation of 5 model proteins on an 80 cm (PDADMAC/PSS)_{2.5} coated capillary. 5 repetitions at -15 kV are shown. Experimental conditions: (PDADMAC/PSS)_{2.5} SMIL coated capillary. Capillary: 50 μ m I.D.; $L = 80$ cm; $l = 71.5$ cm. BGE: 2 M acetic acid, pH 2.2. Flush before each run: BGE 1 bar, 5 min. Sample mixture: 0.2 g/L of CA (1), TI (2), Myo (3), RNase A (4), and Lyz (5) each in BGE. Hydrodynamic co-injection of 0.002% v/v DMF in BGE: half the amount of injection protein mix. Temperature: 25°C. For the coating procedure, see section 2.2.

Analyte electrophoretic heterogeneity

It is possible to quantify the contribution of the heterogeneity of the protein sample from the experiments done on capillaries of different lengths. Indeed, Eq. 17 predicts that if the sample is heterogeneous in terms of electrophoretic mobility, an additional plate height (which increases proportionally to the capillary length to the detector) will be generated. Figure 3 shows the evolution of the constant term in the H vs u curves determined for each protein on different lengths of (PDADMAC/PSS)_{2.5} coated capillaries for the higher injected amount. The data for the 8.5 cm capillary length to the detector was not included because of the very poor separation performance on this length. The overall decrease of the constant terms indicates that the contributions which are inversely proportional to l , in particular H_{inj} , make up most of the constant term, and so there is little impact of sample heterogeneity on plate height. Thus, the model proteins' electrophoretically homogeneous nature is confirmed.

In addition to model proteins, it is interesting to apply this method to the analysis of more polydisperse biomacromolecules such as mAbs, which are known for their charge heterogeneity⁴¹. Following the usual procedure, analyses of a USP mAb at different electric field

strengths were conducted on capillaries of different lengths (30, 40, 66 and 80 cm) and plate heights were determined. Due to their more complex electrophoretic profile, a different method was used to calculate H :

$$H = \frac{lm_2}{m_1^2} \quad (19)$$

where m_1 is the first moment of the residence time distribution which corresponds to the average migration time, and m_2 is the second central moment, which corresponds to the peak variance. The use of the method based on peak width at half height is not adapted to heterogeneous samples because they lead to non-Gaussian peaks.

The constant terms resulting from the H vs u curves (shown in Figure S7B) are plotted against capillary length to the detector in Figure 3, showing a significant increase and overall much higher values compared to the model proteins (see Table S3). This demonstrates that electrophoretic heterogeneity, which is proportional to l , is the main contribution to the constant in the case of the USP mAb, confirming its heterogeneous nature. From the data reported in Figure 3, it can be estimated that, according to Eq. 17, the relative standard deviation of the effective mobilities of USP mAb is approximately equal to 0.8 % (for a slope of 6.41×10^{-5}).

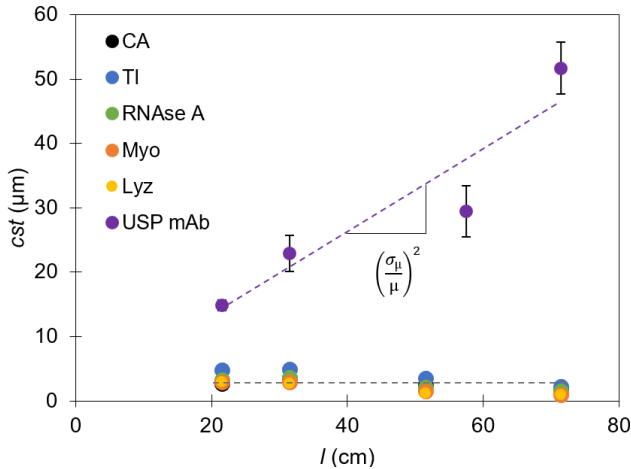


Figure 3. Impact of capillary length on the constant term of the H vs u curve for 5 model proteins on (PDADMAC/PSS)_{2.5} coated capillaries. Plate height was determined using the width at half height for the model proteins and using the moments for the USP mAb. Error bars are \pm one standard deviation on 5 runs for the model proteins, and 3 runs for the mAb. The slope of the USP mAb is 6.41×10^{-5} , which corresponds to $\left(\frac{\sigma_\mu}{\mu}\right)^2$ according to Eq. 17. No polydispersity can be measured for the model proteins. Injected amount: $V_2 = 3.8$ nL. Other experimental conditions as in Figure 2.

Electromigration dispersion or overloading effect

In addition to the extra-column effects described above, another increase in plate height may occur for triangular, asymmetrical peaks. Triangulation is a type of peak deformation which can occur when the solute concentration is high compared to that of the BGE, and for

solutes and BGE co-ions having very different electrophoretic mobilities^{24,42}. This effect is called overloading effect or electromigration dispersion (EMD), and its contribution to plate height for a solute i is expressed as^{24,43}:

$$H_{conc,i} = \left| \frac{2a_i c_i \delta_{inj}}{9} \right| \quad (20)$$

with $a_i = \frac{(r_{iA} - r_{BA})(1 - r_{iA})}{(1 - r_{BA})r_{iA}I}$ and $r_{iA} = \frac{\mu_{eff,i}}{\mu_{eff,A}} \neq 1$, where r_{ji} is the selectivity coefficient between j and i , μ_{eff} the effective mobility, I the ionic strength, c_i the initial solute concentration, δ_{inj} the initial width of the peak, and subscript A designates the co-ion while B designates the counterion. In order to investigate this effect, small molecules were analyzed, as the model proteins all gave rather symmetrical peaks. Three small molecules (creatinine, benzylhydroxylamine and benzylmethylamine) were separated by CE on a (PDADMAC/PSS)_{2.5} SMIL coating and their plate heights were determined for varying electric field strengths (see Figure S8). The usual method to determine plate heights using the width at half height, which relies on the hypothesis that the peak is Gaussian, was no longer adapted. Instead, the Haarhoff-van der Linde (HVL) function in the CEval software, a nonlinear regression function which is useful to fit asymmetrical peaks, was preferred. Thorough comparisons between methods to calculate plate heights were carried out in previous work²⁹.

Table 3. Effect of EMD on slope and constant for benzylhydroxylamine. Experimental conditions: 5-layer (PDADMAC/PSS)_{2.5} SMIL coated capillary. Error bars for each protein are \pm one SD as determined by the jackknife resampling method ($n = 5$). Capillary: 60 cm (51.5 cm to the detector) \times 50 μ m I.D. BGE: 2 M acetic acid, pH 2.2. Flush before each run: BGE 1 bar, 5 min. Hydrodynamic injection: 30 mbar, 6 s. Hydrodynamic co-injection of 0.002% v/v DMF in BGE: 30 mbar, 3 s. Temperature: 25°C. For the coating procedure, see section 2.2.

C (g/L)	C (mmol/L)	p (10^{-3} s)	constant (μ m)
0.2	1.62	0.33 ± 0.07	29.66 ± 0.33
0.04	0.33	0.20 ± 0.25	11.07 ± 0.61
0.02	0.16	0.22 ± 0.26	7.73 ± 0.60
0.01	0.08	0.15 ± 0.33	7.35 ± 0.48

Figure 4 shows the effect of solute concentration on peak shape, which becomes much less triangular as the concentration decreases. The constant decreases with decreasing concentration (see Table 3), which corresponds to the theory of EMD and the equation that describes it (Eq. 20), while the slope remains almost the same. The average slope is even lower than those obtained with the model proteins in the same conditions (1.3×10^{-3} s to 3.6×10^{-3} s, see Table S2). This can be explained by the much lower hydrodynamic radius, and therefore higher diffusion

coefficient, of small molecules compared to proteins (about 10 times ⁴⁴). Indeed, in the assumption that the slope is mostly due to electroosmotic inhomogeneity, Eq. 10 shows that it is inversely proportional to the analyte diffusion coefficient.

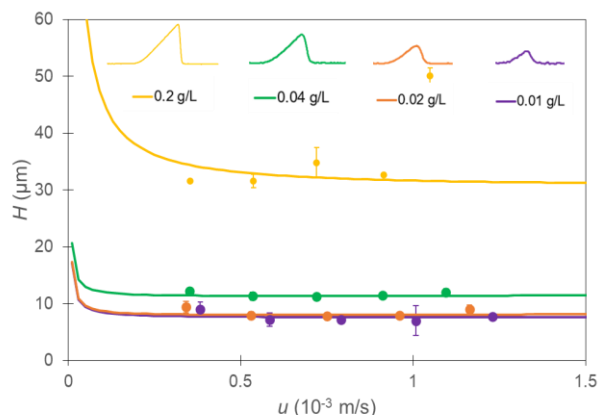


Figure 4. Effect of EMD on H vs u curves and peak shape for different concentrations of benzylhydroxylamine. Peak shapes shown for analyses at -10kV and kept to scale. Plate heights were calculated with the HVL method. Error bars are \pm one standard deviation on 5 runs. The last point of the 0.2 g/L series was not taken into account in the fit. D was determined by Taylor dispersion analysis to be $7.94 \times 10^{-10} \text{ m}^2/\text{s}$. Experimental conditions as in Table 3.

For comparison, separations with a lower concentration of proteins (0.01 g/L each) were also carried out, which resulted in the same plate heights as for the usual concentration (0.02 g/L each), proving that EMD is negligible for model proteins (see Figure S9). Hence, decreasing sample concentration helps to improve separation efficiency when dealing with triangular peak shapes.

Impact of ESI MS detection

In addition to extra-column and sample effects, it is interesting to study the impact of the detector used with the CE on plate height. Until now, all experiments were conducted with UV detection, but MS is often used for identification or even to obtain structural information of electrophoretically separated proteins or proteoforms.

In the current study, experiments were conducted with both UV and MS detections on the same capillary, to avoid inter-capillary variations. The UV detector was placed 8.5 cm from the end of the capillary, while the MS detector was at its end, a difference in effective length which has a negligible impact on the contributions due to injection, detection window, and capillary coiling (less than 0.1 μm difference in H for each). Figure 5 and Table 4 show the H vs u plots and their slopes and constants obtained with each detector.

The constants obtained from the MS detection are close to the ones found for UV detection (0.3 to 1.8 times higher for each protein, see Table 4), and they are similar to the

constants obtained by CE-UV (see Table S2). More notably, the slopes resulting from the MS experiments are consistently higher than ones from the UV (2.2 to 3.1 times) within the CE-UV-MS experiments. Furthermore, the slopes of the H vs u plots of the CE-UV data are slightly lower than the slopes of the UV data in the CE-UV-MS experiments. Several effects might cause additional peak broadening, including hydrodynamic effects, inhomogeneous electrical field strengths, differences in sampling rate, mixing with sheath liquid, protein adsorption outside of the capillary as well as loss of coating at the end of the capillary.

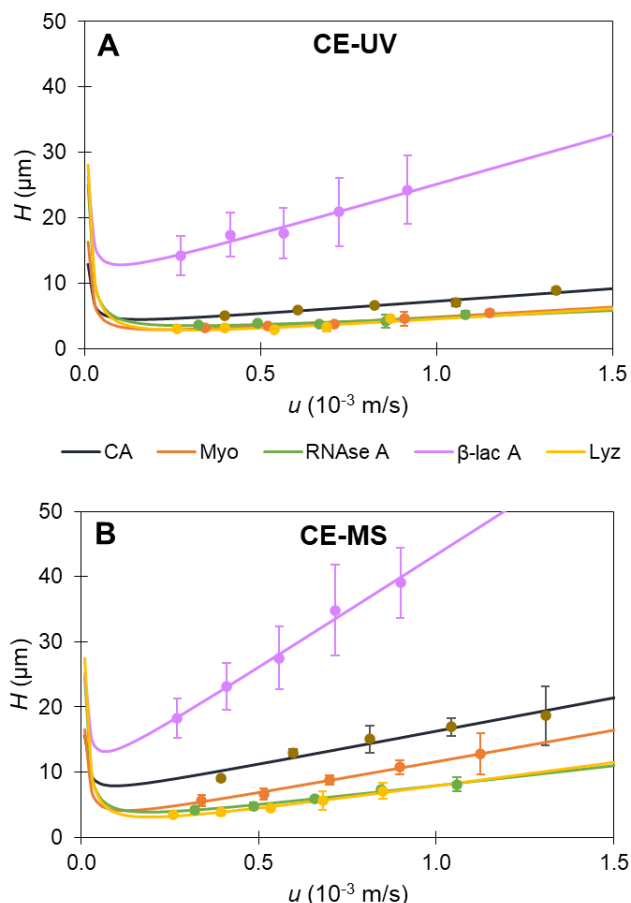


Figure 5. Influence of detection type, UV (A) or MS (B), on the H vs u representations for the separation of 5 model proteins on a 5-layer PDADMAC/PSS SMIL coating. Error bars are \pm one SD on $n=5$ repetitions. Experimental conditions: 5-layer SMIL coated capillary terminating with the polycation PDADMAC. Capillary: 60 cm (51.5 cm to the detector for UV, 60 cm for MS) \times 50 μm I.D. BGE: 2 M acetic acid, pH 2.2. Flush before each run: BGE 1 bar, 5 min. Hydrodynamic injection: 30 mbar, 6 s. Sample mixture: 0.2 g/L of each protein in BGE. Hydrodynamic co-injection of 0.002% v/v DMF in BGE: 30 mbar, 3 s. Temperature: 25°C. Applied voltages: -30 kV, -25 kV, -20 kV, -15 kV, -10 kV. For the coating procedure, see section 2.2.

Differences in the performances of the CE-UV(-MS) compared to CE-UV can be explained by an additional hydrodynamic contribution in the CE-UV-MS experiments

due to the “open system” (no second vials), despite the accurate leveling of the instrument height according to the height level of the interface.

Differences between the UV and MS results within the CE-UV-MS experiments can be due to inhomogeneous electrical field strengths in the interface and the possible adsorption of proteins onto the non-coated glass emitter. Also, the sheath liquid might change the coating properties at the end of the separation capillary. In addition, a (small) dead volume in the glass emitter occurs, where the CE effluent mixes with the sheath liquid ⁴⁵. This dead volume is minimized by etching the capillaries, penetrating them deeply in the emitter ⁴⁶, as well as using a proper high voltage causing a relatively high flow rate ³⁸.

Table 4. Influence of detection type on the slopes and constants of the H vs u curves for the separation of 5 model proteins on a (PDADMAC/PSS)_{2.5} SMIL coating. Error bars for each protein are \pm one SD as determined by the jackknife resampling method ($n = 5$). Errors bars the average are \pm one SD of all the proteins. Experimental conditions as in Figure 5.

	p (10^{-3} s)		constant (μ m)	
	UV	MS	UV	MS
CA	3.92 \pm 0.38	10.29 \pm 1.44	3.24 \pm 0.24	5.92 \pm 1.33
Myo	3.14 \pm 0.27	9.76 \pm 0.26	1.56 \pm 0.20	1.72 \pm 0.25
RNAse A	2.46 \pm 0.45	6.24 \pm 0.30	2.01 \pm 0.25	1.49 \pm 0.15
β -lac A	15.33 \pm 0.77	34.82 \pm 1.43	9.65 \pm 0.53	8.40 \pm 0.6
Lyz	3.33 \pm 0.79	7.36 \pm 0.40	0.95 \pm 0.37	0.30 \pm 0.2
Average	5.64 \pm 5.45	13.69 \pm 11.93	3.48 \pm 3.55	3.56 \pm 3.44

Other sources of error including a possible temperature gradient in the CE-MS system and differences in data acquisition rates ⁴⁷. A study by Zhong et al. simulated mass transport in a micro flow-through vial of a junction-at-the-top CE-MS interface, where the CE effluent is transferred into the MS without dilution or loss of sensitivity, and determined that peak variance increased from 15% to 62% when detected with MS compared to UV ⁴⁷. Therefore, the results obtained in this study seem reasonable and provide interesting insight into the differences in separation efficiency between UV and MS detection. Since the slopes resulting from CE-MS experiments are higher than those from CE-UV, it is more interesting to perform separations at lower electric field strength when using CE-MS.

Conclusion

This work presents a quantitative analysis of the sources of peak dispersion in CE and CE-MS of proteins on SMIL coatings based on a systematic plot of H vs u curves. As expected, contributions linked to the injection and detection window were seen to decrease with the capillary effective length, while the effect of capillary coiling was negligible. Electromigration dispersion was also negligible for proteins, but led to band broadening in the case of small molecules, where triangular peaks were observed. The slope of the H vs u curve, which was shown to be due to electroosmotic inhomogeneity, decreases when the effective length increases, suggesting an irregular distribution of coating defects. Interestingly, we demonstrated in this work that sample heterogeneity did not significantly influence peak broadening for model proteins, unlike the USP mAb for which it was the main contribution to plate height. To our knowledge, this is the first time that the contribution of sample polydispersity can be clearly quantified and deciphered from other sources of peak broadening. Also for the first time, a thorough investigation of separation performance resulting from UV or MS detection was conducted, showing slightly lower separation performance with the MS detection compared to the UV (higher slopes p), which can be explained by differences in experimental setup. This new information on peak dispersion inherent to MS detection may give some leads as to how its performance could be improved in the future. On the whole, the 5-layer PDADMAC/PSS SMIL on an 80 cm long capillary led to up to 941 000 plates/m with high repeatability ($\%RSD(t_m) < 0.29$), which is not so far from the maximum value predicted in the case of an ideal separation controlled only by axial diffusion (1.65 million plates/m with $D = 7.4 \times 10^{-11} \text{ m}^2\text{s}^{-1}$). In these optimized conditions, the SMIL coatings could be used for the analysis of a mAb. However, it should be kept in mind that mAbs cannot be used to optimize coating conditions using the H vs u curves because their heterogeneity impacts the constant term, and that evaluating coating performance requires model proteins with low heterogeneity.

AUTHOR INFORMATION

Corresponding Author

Hervé Cottet. Phone: +33 4 67 14 34 27. Fax: +33 4 67 63 10 46. E-mail: herve.cottet@umontpellier.fr. ORCID Hervé Cottet: 0000-0002-6876-175X

Author Contributions

The manuscript was written through contributions of all authors.

ACKNOWLEDGMENT

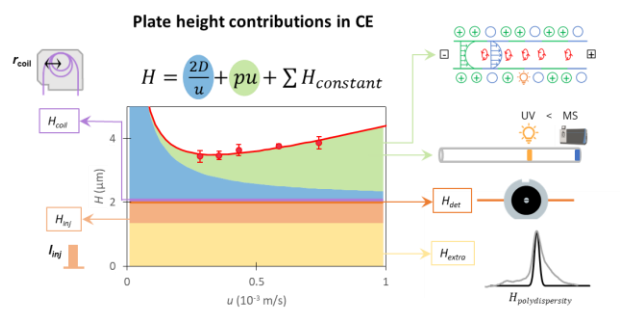
This work was done as part of a PRCI in collaboration with German partners from the University of Aalen, Germany (ANR-DFG SMIL E, ANR-20-C E 92-0021-01).

REFERENCES

- (1) Walsh, G. Biopharmaceutical Benchmarks 2014. *Nat Biotechnol* **2014**, 32 (10), 992–1000. <https://doi.org/10.1038/nbt.3040>.

- (2) Baldo, B. A. Monoclonal Antibodies Approved for Cancer Therapy. In *Safety of Biologics Therapy*; Springer International Publishing: Cham, 2016; pp 57–140. https://doi.org/10.1007/978-3-319-30472-4_3.
- (3) Berkowitz, S. A.; Engen, J. R.; Mazzeo, J. R.; Jones, G. B. Analytical Tools for Characterizing Biopharmaceuticals and the Implications for Biosimilars. *Nat Rev Drug Discov* **2012**, *11* (7), 527–540. <https://doi.org/10.1038/nrd3746>.
- (4) Staub, A.; Guilleme, D.; Schappler, J.; Veuthey, J.-L.; Rudaz, S. Intact Protein Analysis in the Biopharmaceutical Field. *Journal of Pharmaceutical and Biomedical Analysis* **2011**, *55* (4), 810–822. <https://doi.org/10.1016/j.jpba.2011.01.031>.
- (5) Shi, Y.; Li, Z.; Qiao, Y.; Lin, J. Development and Validation of a Rapid Capillary Zone Electrophoresis Method for Determining Charge Variants of mAb. *Journal of Chromatography B* **2012**, *906*, 63–68. <https://doi.org/10.1016/j.jchromb.2012.08.022>.
- (6) Moritz, B.; Schnaible, V.; Kiessig, S.; Heyne, A.; Wild, M.; Finkler, C.; Christians, S.; Mueller, K.; Zhang, L.; Furuya, K.; Hassel, M.; Hamm, M.; Rustandi, R.; He, Y.; Solano, O. S.; Whitmore, C.; Park, S. A.; Hansen, D.; Santos, M.; Lies, M. Evaluation of Capillary Zone Electrophoresis for Charge Heterogeneity Testing of Monoclonal Antibodies. *Journal of Chromatography B* **2015**, *983–984*, 101–110. <https://doi.org/10.1016/j.jchromb.2014.12.024>.
- (7) He, Y.; Isele, C.; Hou, W.; Ruesch, M. Rapid Analysis of Charge Variants of Monoclonal Antibodies with Capillary Zone Electrophoresis in Dynamically Coated Fused-Silica Capillary: Electrodriven Separations. *J. Sep. Science* **2011**, *34* (5), 548–555. <https://doi.org/10.1002/jssc.201000719>.
- (8) He, Y.; Lacher, N. A.; Hou, W.; Wang, Q.; Isele, C.; Starkey, J.; Ruesch, M. Analysis of Identity, Charge Variants, and Disulfide Isomers of Monoclonal Antibodies with Capillary Zone Electrophoresis in an Uncoated Capillary Column. *Anal. Chem.* **2010**, *82* (8), 3222–3230. <https://doi.org/10.1021/ac9028856>.
- (9) Espinosa- De La Garza, C. E.; Perdomo-Abúndez, F. C.; Padilla-Calderón, J.; Uribe-Wiechers, J. M.; Pérez, N. O.; Flores-Ortiz, L. F.; Medina-Rivero, E. Analysis of Recombinant Monoclonal Antibodies by Capillary Zone Electrophoresis: CE and CEC. *Electrophoresis* **2013**, *34* (8), 1133–1140. <https://doi.org/10.1002/elps.201200575>.
- (10) Bohoyo, D.; Le Potier, I.; Rivière, C.; Klafki, H.; Wiltfang, J.; Taverna, M. A Quantitative CE Method to Analyse Tau Protein Isoforms Using Coated Fused Silica Capillaries: Electrodriven Separations. *J. Sep. Sci.* **2010**, *33* (8), 1090–1098. <https://doi.org/10.1002/jssc.200900713>.
- (11) Wiesner, R.; Zagst, H.; Lan, W.; Bigelow, S.; Holper, P.; Hübner, G.; Josefsson, L.; Lancaster, C.; Lo, L.; Löfner, C.; Lu, H.; Neusüß, C.; Rüttiger, C.; Schlecht, J.; Schürle, P.; Selsam, A.; Burg, D. van der; Wang, S.-C.; Zhu, Y.; Wätzig, H.; Griend, C. S. de. An Interlaboratory Capillary Zone electrophoresis-UV Study of Various Monoclonal Antibodies, Instruments, and E-aminocaproic Acid Lots. **2023**, *44* (15–16), 1247–1257. <https://doi.org/10.1002/elps.202200284>.
- (12) Meudt, M.; Pannek, M.; Glogowski, N.; Higel, F.; Thanisch, K.; Knappe, M. J. CE Methods for Charge Variant Analysis of mAbs and Complex Format Biotherapeutics. *Electrophoresis* **2024**, 1–12. <https://doi.org/10.1002/elps.202300170>.
- (13) Katayama, H.; Ishihama, Y.; Asakawa, N. Stable Cationic Capillary Coating with Successive Multiple Ionic Polymer Layers for Capillary Electrophoresis. *Anal. Chem.* **1998**, *70* (24), 5272–5277. <https://doi.org/10.1021/ac980522l>.
- (14) Pei, L.; Lucy, C. A. Insight into the Stability of Poly(Diallyldimethylammoniumchloride) and Polybrene Poly Cationic Coatings in Capillary Electrophoresis. *J. Chromatogr. A* **2014**, *1365*, 226–233. <https://doi.org/10.1016/j.chroma.2014.09.013>.
- (15) Stefanik, O.; Majerova, P.; Kovac, A.; Mikus, P.; Piestansky, J. Capillary Electrophoresis in the Analysis of Therapeutic Peptides—A Review. *Electrophoresis* **2023**, *45* (1–2), 120–164. <https://doi.org/10.1002/elps.202300141>.
- (16) Kašička, V. Recent Developments in Capillary and Microchip Electro-separations of Peptides (2021–Mid-2023). *Electrophoresis* **2023**, *45* (1–2), 165–198. <https://doi.org/10.1002/elps.202300152>.
- (17) Štěpánová, S.; Kašička, V. Applications of Capillary Electromigration Methods for Separation and Analysis of Proteins (2017–Mid 2021) – A Review. *Anal. Chim. Acta* **2022**, *1209*, 339447. <https://doi.org/10.1016/j.aca.2022.339447>.
- (18) Maráková, K.; Opetová, M.; Tomašovský, R. Capillary Electrophoresis-mass Spectrometry for Intact Protein Analysis: Pharmaceutical and Biomedical Applications (2018–March 2023). *J. Sep. Sci.* **2023**, *46* (15). <https://doi.org/10.1002/jssc.202300244>.
- (19) Huhn, C.; Ramautar, R.; Wührer, M.; Somsen, G. W. Relevance and Use of Capillary Coatings in Capillary Electrophoresis-Mass Spectrometry. *Anal. Bioanal. Chem.* **2010**, *396* (1), 297–314. <https://doi.org/10.1007/s00216-009-3193-y>.
- (20) Balaguer, E.; Demelbauer, U.; Pelzing, M.; Sanz-Nebot, V.; Barbosa, J.; Neusüß, C. Glycoform Characterization of Erythropoietin Combining Glycan and Intact Protein Analysis by Capillary Electrophoresis – Electrospray – Time-of-flight Mass Spectrometry. *Electrophoresis* **2006**, *27* (13), 2638–2650. <https://doi.org/10.1002/elps.200600075>.
- (21) Biais, M.; Gahoual, R.; Said, N.; Beck, A.; Leize-Wagner, E.; François, Y.-N. Glycoform Separation and Characterization of Cetuximab Variants by Middle-up Off-Line Capillary Zone Electrophoresis-UV/Electrospray Ionization-MS. *Anal. Chem.* **2015**, *87* (12), 6240–6250. <https://doi.org/10.1021/acs.analchem.5b00928>.
- (22) Haselberg, R.; Brinks, V.; Hawe, A.; de Jong, G. J.; Somsen, G. W. Capillary Electrophoresis-Mass Spectrometry Using Noncovalently Coated Capillaries for the Analysis of Biopharmaceuticals. *Anal. Bioanal. Chem.* **2011**, *400* (1), 295–303. <https://doi.org/10.1007/s00216-011-4738-4>.
- (23) Minárik, M.; Gaš, B.; Rizzi, A.; Kenndler, E. Plate Height Contribution from Wall Adsorption in Capillary Zone Electrophoresis of Proteins. *Journal of Capillary Electrophoresis* **1995**, *2* (2), 89–96.
- (24) Kenndler, E. Capillary Zone Electrophoresis in the Absence of Electroosmotic Flow. In *High-Performance Capillary Electrophoresis*; 1998; Vol. 146, pp 34–53.
- (25) Leclercq, L.; Renard, C.; Martin, M.; Cottet, H. Quantification of Adsorption and Optimization of Separation of Proteins in Capillary Electrophoresis. *Anal. Chem.* **2020**, *92* (15), 10743–10750. <https://doi.org/10.1021/acs.analchem.0c02012>.
- (26) Schure, M. R.; Lenhoff, A. M. Consequences of Wall Adsorption in Capillary Electrophoresis: Theory and Simulation. *Anal. Chem.* **1993**, *65* (21), 3024–3037. <https://doi.org/10.1021/ac00069a015>.
- (27) Ghosal, S. Fluid Mechanics of Electroosmotic Flow and Its Effect on Band Broadening in Capillary Electrophoresis. *Electrophoresis* **2004**, *25* (2), 214–228. <https://doi.org/10.1002/elps.200305745>.
- (28) Dhellemmes, L.; Leclercq, L.; Lichtenauer, L.; Höchsmann, A.; Leitner, M.; Ebner, A.; Martin, M.; Neusüß, C.; Cottet, H. Dual Contributions of Analyte Adsorption and Electroosmotic Inhomogeneity to Separation Efficiency in Capillary Electrophoresis of Proteins. *Anal. Chem.* **2024**. <https://doi.org/10.1021/acs.analchem.4c00274>.

- (29) Dhellemmes, L.; Leclercq, L.; Höchsmann, A.; Neusüß, C.; Biron, J.-P.; Roca, S.; Cottet, H. Critical Parameters for Highly Efficient and Reproducible Polyelectrolyte Multilayer Coatings for Protein Separation by Capillary Electrophoresis. *Journal of Chromatography A* **2023**, *1695*, 463912. <https://doi.org/10.1016/j.chroma.2023.463912>.
- (30) Gaš, B.; Kenndler, E. Dispersive Phenomena in Electromigration Separation Methods. *Electrophoresis* **2000**, *21* (18), 3888–3897. [https://doi.org/10.1002/1522-2683\(200012\)21:18<3888::AID-ELPS3888>3.0.CO;2-D](https://doi.org/10.1002/1522-2683(200012)21:18<3888::AID-ELPS3888>3.0.CO;2-D).
- (31) Grushka, E. Effect of Hydrostatic Flow on the Efficiency in Capillary Electrophoresis. *Journal of Chromatography A* **1991**, *559* (1–2), 81–93. [https://doi.org/10.1016/0021-9673\(91\)80060-T](https://doi.org/10.1016/0021-9673(91)80060-T).
- (32) Kašička, V.; Prusik, Z.; Gaš, B.; Štědrý, M. Contribution of Capillary Coiling to Zone Dispersion in Capillary Zone Electrophoresis. *Electrophoresis* **1995**, *16* (1), 2034–2038. <https://doi.org/10.1002/elps.11501601332>.
- (33) Wicar, S.; Vilenchik, M.; Belenkii, A.; Cohen, A. S.; Karger, B. L. Influence of Coiling on Performance in Capillary Electrophoresis Using Open Tubular and Polymer Network Columns. *J. Micro. Sep.* **1992**, *4* (4), 339–348. <https://doi.org/10.1002/mcs.1220040408>.
- (34) Xuan, X.; Li, D. Band-Broadening in Capillary Zone Electrophoresis with Axial Temperature Gradients. *Electrophoresis* **2005**, *26* (1), 166–175. <https://doi.org/10.1002/elps.200406141>.
- (35) Potoček, B.; Gaš, B.; Kenndler, E.; Štědrý, M. Electroosmosis in Capillary Zone Electrophoresis with Non-Uniform Zeta Potential. *Journal of Chromatography A* **1995**, *709* (1), 51–62. [https://doi.org/10.1016/0021-9673\(95\)00109-Z](https://doi.org/10.1016/0021-9673(95)00109-Z).
- (36) Gaš, B.; Štědrý, M.; Kenndler, E. Contribution of the Electroosmotic Flow to Peak Broadening in Capillary Zone Electrophoresis with Uniform Zeta Potential. *Journal of Chromatography A* **1995**, *709* (1), 63–68. [https://doi.org/10.1016/0021-9673\(95\)00068-X](https://doi.org/10.1016/0021-9673(95)00068-X).
- (37) Dubský, P.; Ördögová, M.; Malý, M.; Riesová, M. CEval: All-in-One Software for Data Processing and Statistical Evaluations in Affinity Capillary Electrophoresis. *Journal of Chromatography A* **2016**, *1445*, 158–165. <https://doi.org/10.1016/j.chroma.2016.04.004>.
- (38) Schlecht, J.; Stolz, A.; Hofmann, A.; Gerstung, L.; Neusüß, C. nanoCEasy: An Easy, Flexible, and Robust Nanoflow Sheath Liquid Capillary Electrophoresis-Mass Spectrometry Interface Based on 3D Printed Parts. *Anal. Chem.* **2021**, *93* (14), 14593–14598. <https://doi.org/10.1021/acs.analchem.1c03213>.
- (39) Graul, T. W.; Schlenoff, J. B. Capillaries Modified by Polyelectrolyte Multilayers for Electrophoretic Separations. *Anal. Chem.* **1999**, *71* (18), 4007–4013. <https://doi.org/10.1021/ac990277l>.
- (40) Roca, S.; Dhellemmes, L.; Leclercq, L.; Cottet, H. Polyelectrolyte Multilayers in Capillary Electrophoresis. *ChemPlusChem* **2022**, *87* (4), 14593–14598. <https://doi.org/10.1002/cplu.202200028>.
- (41) Kumar, R.; Guttman, A.; Rathore, A. S. Applications of Capillary Electrophoresis for Biopharmaceutical Product Characterization. *Electrophoresis* **2022**, *43* (1–2), 143–166. <https://doi.org/10.1002/elps.202100182>.
- (42) Mikkers, F. E. P.; Everaerts, F. M.; Verheggen, Th. P. E. M. Concentration Distributions in Free Zone Electrophoresis. *Journal of Chromatography A* **1979**, *169*, 1–10. [https://doi.org/10.1016/0021-9673\(75\)85028-X](https://doi.org/10.1016/0021-9673(75)85028-X).
- (43) Reijenga, J. C.; Kenndler, E. Computational Simulation of Migration and Dispersion in Free Capillary Zone Electrophoresis. *Journal of Chromatography A* **1994**, *659* (2), 403–415. [https://doi.org/10.1016/0021-9673\(94\)85083-6](https://doi.org/10.1016/0021-9673(94)85083-6).
- (44) Hulse, W. L.; Forbes, R. T. A Nanolitre Method to Determine the Hydrodynamic Radius of Proteins and Small Molecules by Taylor Dispersion Analysis. *International Journal of Pharmaceutics* **2011**, *411* (1–2), 64–68. <https://doi.org/10.1016/j.ijpharm.2011.03.040>.
- (45) Wojcik, R.; Dada, O. O.; Sadilek, M.; Dovichi, N. J. Simplified Capillary Electrophoresis Nanospray Sheath-Flow Interface for High Efficiency and Sensitive Peptide Analysis: Capillary Electrophoresis Electrospray Interface. *Rapid Commun. Mass Spectrom.* **2010**, *24* (17), 2554–2560. <https://doi.org/10.1002/rcm.4672>.
- (46) Höcker, O.; Montealegre, C.; Neusüß, C. Characterization of a Nanoflow Sheath Liquid Interface and Comparison to a Sheath Liquid and a Sheathless Porous-Tip Interface for CE-ESI-MS in Positive and Negative Ionization. *Anal. Bioanal. Chem.* **2018**, *410* (21), 5265–5275. <https://doi.org/10.1007/s00216-018-1179-3>.
- (47) Zhong, X.; Maxwell, E. J.; Chen, D. D. Y. Mass Transport in a Micro Flow-Through Vial of a Junction-at-the-Tip Capillary Electrophoresis-Mass Spectrometry Interface. *Anal. Chem.* **2011**, *83* (12), 4916–4923. <https://doi.org/10.1021/ac200636y>.



For Table of Contents Only
